3-Aroyl-1,4-diarylpyrroles Inhibit Chronic Myeloid Leukemia Cell Growth through an Interaction with Tubulin

Giuseppe La Regina,[†] Ruoli Bai,[‡] Antonio Coluccia,[†] Valeria Famiglini,[†] Sara Passacantilli,[†] Valentina Naccarato,[†] Giorgio Ortar,[†]Carmela Mazzoccoli,[≠] Vitalba Ruggieri,[≠] Francesca Agriesti,[≠] Claudia Piccoli,[≠,æ] Tiziana Tataranni,[≠] Marianna Nalli,[†] Andrea Brancale,[∞] Stefania Vultaggio,[◆] Ciro Mercurio,[◆] Mario Varasi,[◆] Concetta Saponaro,[○] Sara Sergio,[○] Michele Maffia,[○] Addolorata Maria Luce Coluccia,[○] Ernest Hamel,[‡] and Romano Silvestri,[*,†]

[†]Institut Pasteur Italy - Cenci Bolognetti Foundation, Dipartimento di Chimica e Tecnologie del Farmaco, Sapienza Università di Roma, Piazzale Aldo Moro 5, I-00185 Roma, Italy

[‡]Screening Technologies Branch, Developmental Therapeutics Program, Division of Cancer Treatment and Diagnosis, Frederick National Laboratory for Cancer Research, National Cancer Institute, National Institutes of Health, Frederick, Maryland 21702, USA

[≠]Laboratory of Pre-clinical and Translational Research, IRCCS-CROB, Referral Cancer Center of Basilicata, Rionero in Vulture, Italy

[æ]Department of Clinical and Experimental Medicine, University of Foggia, Foggia, Italy

[∞]Cardiff School of Pharmacy and Pharmaceutical Sciences, Cardiff University, King Edward VII Avenue, Cardiff, CF10 3NB, UK

[○]Clinical Proteomics, Polo Oncologico Giovanni Paolo II, ASL - University of Salento, Piazza Muratore 1, 73100 Lecce, Italy

[◆] Experimental Therapeutics Unit, IFOM-the FIRC Institute of Molecular Oncology Foundation, Via Adamello 16, I-20139 Milano, Italy

KEYWORDS cancer, tubulin, chronic myeloid leukemia, synthesis, 3-aroyl-1,4-diarylpyrrole

ABSTRACT: We designed 3-aroyl-1,4-diarylpyrrole (ARDAP) derivatives as potential anticancer agents having different substituents at the 1- or 4-phenyl ring. ARDAP compounds exhibited potent inhibition of tubulin polymerization, binding of colchicine to tubulin and cancer cell growth. ARDAP derivative **10** inhibited the proliferation of BCR/ABL-expressing KU812 and LAMA84 cells from chronic myeloid leukemia (CML) patients in blast crisis and of hematopoietic cells ectopically expressing the imatinib mesylate (IM)-sensitive KBM5-WT or its IM-resistant KBM5-T315I mutation. Compound **10** minimally affected the proliferation of normal blood cells, indicating that it may be a promising agent to overcome broad tyrosine kinase inhibitor resistance in relapsed/refractory CML patients. Compound **10** significantly decreased CML proliferation by inducing G2/M phase arrest and apoptosis via a mitochondria-dependent pathway. ARDAP **10** augmented the cytotoxic effects of IM in human CML cells. Compound **10** represents a robust lead compound to develop tubulin inhibitors with potential as novel treatments for CML.

Chronic myeloid leukemia (CML) is a myeloproliferative disease with an incidence of 1.8 new cases per 100,000 men and women per year.[1] The hallmark of CML is the reciprocal translocation t(9;22)(q34;q11) (*i.e.*, the Philadelphia chromosome, Ph) encoding for the hybrid protein BCR/ABL, a tyrosine kinase with leukemogenic potential.[2,3] At present, imatinib mesylate (IM, Gleevec), an inhibitor of both the BCR/ABL and c-ABL tyrosine kinases, represents the treatment of choice for CML, inducing stable clinical remissions in more than 80% of newly-diagnosed patients.

However, point mutations in the catalytic domain of the BCR/ABL oncoprotein[4,5] or *bcr/abl* gene amplification[6] can select IM-resistant clones in CML patients leading to a fatal blast crisis phase. Among the reported BCR/ABL point mutations, T315I (resulting in substitution of a threonine for an isoleucine residue at the 'gatekeeper' position 315) is of particular interest because it also provides resistance to clinically useful second-generation tyrosine kinase inhibitors (TKIs) such as nilotinib, dasatinib and bosutinib.[7] Therefore, there is a pressing need for devising novel combination regimens aimed at overcoming TKI-resistance in CML cells.

Microtubules are an attractive target for the development of effective anti-leukemia agents.[8,9] Evidence has accumulated correlating inhibition of tubulin polymerization and leukemic cell proliferation.[10-14] The activity of colchicine site agents in CML has not been adequately explored. In continuing our studies on tubulin targeting agents, we designed new 3-aroyl-1,4-diarylpyrrole (ARDAP) derivatives (Chart 1, Table 1).

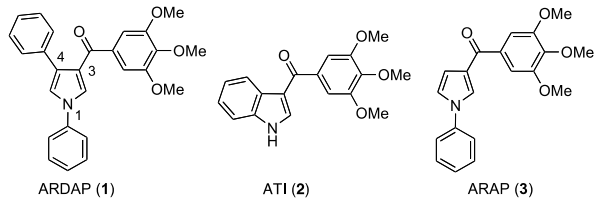

Chart 1. ARDAP (**1**), ATI (**2**) and ARAP (**3**) derivatives.

Docking studies on ARDAP prototype **1** showed that the proposed binding mode was significantly different from those of its parent compounds ATI **2**[15] and ARAP **3**.[16] However, the three compounds all shared the key interactions of the trimethoxyphenyl moiety with the βCys241 of tubulin (Figure 1). Observing the binding mode of ARDAP **1**, we noticed that the *N*-phenyl pyrrole group of **1** was placed in the same position as the indole ring of **2**, while the other ARDAP phenyl ring occupied the same area as colchicine ring B.[17] Based on these observations, we decided to investigate this new scaffold in search of novel tubulin binding agents. We planned the synthesis of a group of ARDAP derivatives bearing phenyl or substituted-phenyl groups at positions 1 and 4 of the pyrrole nucleus (**4-16**, Table 1). In this study, we introduced on the phenyl rings substituents that were associated with the best biological activity in the ARAP series.[16]

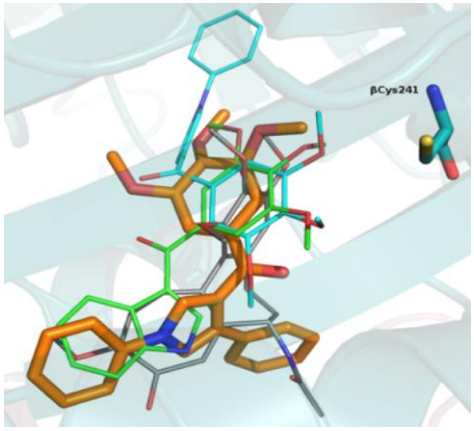

Figure 1. Proposed binding modes for **1** (orange stick), **2** (green), **3** (cyan) and colchicine (gray) in the colchicine site.

The new ARDAP derivatives were synthesized starting from chalcones **25-31**, which were converted to the corresponding pyrrole derivatives **32**[16] or **33-39** with *p*-toluenesulfonylmethyl isocyanide (TosMIC). ARDAP compounds **1**, **4-6**, **8**, **9**, **12**, **13**, **15**, and **16** were obtained by reacting **32**[16] or **33-39** with the appropriate boronic acid **40**, **42**, **43**, **45** or **46**. Reduction of **47** with Pd/C-H_2 (1 atm) gave the ARDAP derivative **7**. Tin(II) chloride treatment of nitro derivatives **48-50** furnished ARDAPs **10** and **14** and compound **51**, respectively. The latter compound was converted to ARDAP **11** with sodium nitrite in tetrafluoroboric acid. Reagents and reaction conditions are summarized in the Scheme 1 legend.

In an initial screen, ARDAP **1** proved to be superior to **3** as an inhibitor of MCF-7 cell growth (Table 1). Besides the ability to inhibit tubulin polymerization, for which they were originally designed, we found that ARDAP compounds augment IM-mediated apoptotic effects in BCR/ABL$^+$ CML cells obtained from patients in blast crisis.

ARDAP derivatives inhibited tubulin polymerization at micro- or submicromolar (**4**, **6, 7**, **9** and **15**) concentrations, as compared with colchicine (IC_{50} = 3.2 μM) and combretastatin A-4 (CSA4) (IC_{50} = 1.0 μM). Most ARDAP compounds potently inhibited the growth of MCF-7 cells. ARDAPs **4**, **7**, **10**, **15** and **16** exhibited IC_{50} values ≤30 nM.

Table 1. Inhibition of Tubulin Polymerization, Growth of MCF-7 Human Breast Carcinoma Cells, and Colchicine Binding by ARDAPs 4-16 and References 3, Colchicine and CSA4.[a]

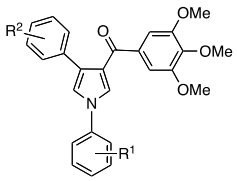

1, 4-16

compd	R^1	R^2	Tubulin[b] IC_{50} ± SD (μM)	MCF-7[c] IC_{50} ± SD (nM)	Inh. Colch. Binding[d] (% ± SD)
1	H	H	1.1 ± 0.1	35 ± 7	66 ± 1
4	H	2-F	0.58 ± 0.02	30 ± 7	72 ± 4
5	H	3-Me	1.6 ± 0.04	450 ± 70	5.7 ± 5
6	H	3-F	0.63 ± 0.004	57 ± 2	53 ± 0.7
7	H	3-NH_2	0.39 ± 0.05	28 ± 3	57 ± 0.7
8	H	4-Me	2.2 ± 0.1	280 ± 40	24 ± 0.07
9	H	4-F	0.76 ± 0.1	78 ± 4	47 ± 4
10	H	4-NH_2	1.2 ± 0.1	9.0 ± 2	81 ± 2
11	2-F	H	2.0 ± 0.1	85 ± 7	29 ± 5
12	3-Me	H	1.7 ± 0.09	120 ± 0	82 ± 2
13	3-F	H	2.9 ± 0.3	350 ± 90	42 ± 0.5
14	3-NH_2	H	1.1 ± 0.08	74 ± 6	82 ± 4
15	4-Me	H	0.88 ± 0.03	30 ± 0	79 ± 0.1
16	4-F	H	1.3 ± 0.1	15 ± 5	62 ± 2
3[e]	—	—	1.5 ± 0.2	700 ± 200	80 ± 2
Colch	—	—	3.2 ± 0.4	5 ± 1	—
CSA4	—	—	1.0 ± 0.1[f,g]	13 ± 3	98 ± 0.6

[a]Experiments were performed in triplicate. [b]Inhibition of tubulin polymerization. Tubulin was at 10 μM in the assembly assay. [c]Inhibition of growth of MCF-7 human breast carcinoma cells. [d]Inhibition of [^{3}H]colchicine binding: tubulin, [^{3}H]colchicine, inhibitor at 1:5:5 μM. [e]Lit.[16] [f]CSA4 yielded an IC_{50} = 0.65 μM in an assay contemporaneous with the evaluations of ARDAPs **5** and **7**, in which a different tubulin preparation was used. [g]CSA4 yielded an IC_{50} of 0.79 μM in an assay contemporaneous with the evaluations of **4**, **6** and **9**, in which a different tubulin preparation was used.

Compound **10** was the most potent MCF-7 cell growth inhibitor within the series with an IC_{50} of 9 nM. In general, inhibition of colchicine binding correlated with inhibition of tubulin polymerization and MCF-7 cell growth. The best tubulin assembly inhibitor **7** (IC_{50} = 0.39 μM) inhibited the growth of MCF-7 cells with an IC_{50} of 28 nM and colchicine binding by 57%. The best MCF-7 cell growth inhibitor **10** (IC_{50} = 9 nM) inhibited tubulin polymerization with an IC_{50} of 1.2 μM and colchicine binding by 81% (Table 1). As inhibitors of the ovarian carcinoma cell lines OVCAR-8 and its cognate P-glycoprotein (Pgp) overexpressing line NCI/ADR-RES, compound **7** yielded IC_{50} values of 190 and 110 nM, and **16** of 180 and 110 nM, respectively. With the exception of CSA-4, the reference colchicine, vinorelbine, vinblastine and paclitaxel were quite weak inhibitors of the MDR cell line (Table 1S, Supporting Information).

Scheme 1. Synthesis of Compounds 1 and 4-16[a]

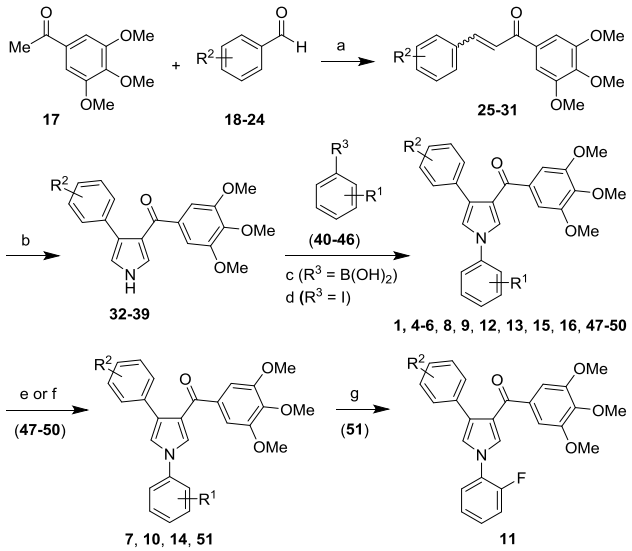

ARDAPs **1** and **4-16**: see Table 1. **18**, **25**: R^2 = 2-F; **19, 26**: R^2 = 3-Me; **20**, **27**: R^2 = 3-F; **21**, **28**: R^2 = 3-NO_2; **22**, **29**: R^2 = 4-Me; **23**, **30**: R^2 = 4-F; **24**, **31**: R^2 = 4-NO_2; **32**: R^2 = H; **33**: R^2 = 2-F; **34**: R^2 = 3-Me; **35**: R^2 = 3-F; **36**: R^2 = 3-NO_2; **37**: R^2 = 4-Me; **38**: R^2 = 4-F; **39**: R^2 = 4-NO_2; **40**: R^1 = H, R^3 = $B(OH)_2$; **41**: R^1 = 2-NO_2, R^3 = I; **42**: R^1 = 3-Me, R^3 = $B(OH)_2$; **43**: R^1 = 3-F, R^3 = $B(OH)_2$; **44**: R^1 = 3-NO_2, R^3 = I; **45**: R^1 = 4-Me, R^3 = $B(OH)_2$; **46**: R^1 = 4-F, R^3 = $B(OH)_2$; **47**: R^1 = H, R^2 = 3-NO_2; **48**: R^1 = H, R^2 = 4-NO_2; **49**: R^1 = 2-NO_2, R^2 = H; **50**: R^1 = 3-NO_2, R^2 = H; **51**: R^1 = 2-NH_2, R_2 = H.

[a]Reagents and reaction conditions. (a) NaOH, EtOH, 25 °C, 24 h, 59-89%; (b) TosMIC, NaH, DMSO/Et_2O, 25 °C, 4 h, Ar, 21-84%; (c) (**1**, **4**, **5**, **8**, **9**, **12**, **13**, **15**, **16**, **47** and **48**) boronic acid **40**, **42**, **43**, **45** or **46**, $Cu(AcO)_2$, Et_3N, DCE, reflux, Ar, 4-72%; (d) (**49** and **50**) **41** or **44**, CuBr, Cs_2CO_3, quinoline *N*-oxide, DMSO, 65 °C, 6 h, Ar, 9 and 34%; (e) (**7**) H_2, Pd/C, MeOH, 1 atm, 25 °C, 2 h, 82%; (f) (**10**, **14** and **51**) $SnCl_2.2H_2O$, MeCOOEt, reflux, 6 h, 47-60%; (g) $NaNO_2$, HBF_4, 0 °C, 1 h, 13%.

Compounds **7**, **10** and **16** were evaluated for growth inhibition of the KYSE150 (esophageal squamous cell), THP-1 (acute monocytic leukemia), NB4 (acute promyelocytic leukemia), HT-29 (human colorectal adenocarcinoma), HCT116 (colon cancer) and HepG2 (liver hepatocellular) cell lines (Table 2S, Supporting Information). Derivative **10** was found to be the most potent compound, with IC_{50} values ranging from 20 nM (KYSE150 and HCT116) to 46 nM (HepG2).

The most potent ARDAP derivative **10** was investigated for efficacy with BCR/ABL-expressing cells established *in vitro* from CML patients in blast crisis (KU812 and LAMA 84) compared with previously reported colchicine site binders 2-(*1H*-imidazol-1-yl)-3-((3,4,5-trimethoxyphenyl)thio)-*1H*-indole[19] (**52**) and (1-(3-aminophenyl)-*1H*-pyrrol-3-yl)(3,4,5-trimethoxyphenyl)methanone[16] (**53**). While derivatives **52** and **53** inhibited CML cell growth (IC_{50}) at concentrations ranging from 28 to 35 nM, ARDAP derivative **10** was the most potent compound (IC_{50} = 12 and 14 nM, respectively) (Table 3S and Figure 3S, Supporting Information). These results demonstrate that high cytotoxicity can occur with compounds belonging to this new class of compounds.

A dose-dependent inhibition of proliferation was observed for KU812 and LAMA84 cells exposed to increasing doses of **10** for 48 h, as assessed by MTT assays. Compound **10** inhibited CML cell growth by 50% at 12 nM. At such nanomolar concentrations, **10** minimally affected normal blood cells. Of note, peripheral blood mononuclear cells (PBMCs) isolated from healthy donors remained substantially insensitive to **10** up to 1 μM (Figure 2).

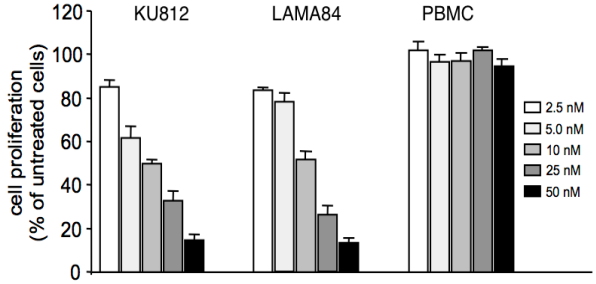

Figure 2. Compound **10** decreased CML cell proliferation at nanomolar concentrations without affecting normal PBMCs. Experiments were performed in triplicate.

Based on the above data, by virtue of its anti-leukemic potential, we extended the analysis of biological effects of **10** to proliferation and viability of IM-sensitive KBM5 and IM-resistant KBM5-T315I cells (Figure 3). By performing MTT assays, we found that **10** dose-dependently blocked growth of KBM5 and KBM5-T315I cells with similar average IC_{50} values of 15 and 18 nM, respectively. The anti-leukemic activity of **10** in BCR/ABL^+ cells expressing the T315I gatekeeper mutation indicated that the drug may be a promising agent to overcome broad TKI-resistance in relapsed/refractory CML patients.

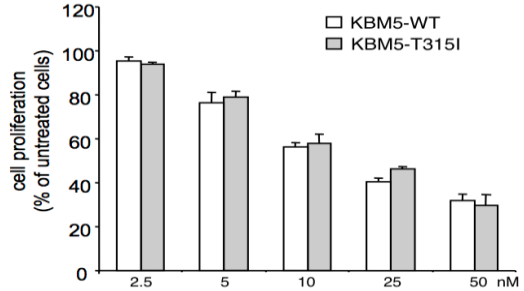

Figure 3. Cytotoxicity of **10** on CML cells ectopically expressing the IM-sensitive wild type KBM5-WT or its IM-resistant KBM5-T315I mutation. Experiments were performed in triplicate.

A rapid collapse of mitochondrial transmembrane potential was detected in KU812 cells exposed to 100 nM **10** for 8 h, to a greater extent as compared with those exposed to IM (100 nM for 8 h), as a consequence of the opening of permeability transition pores that accumulate a fluorescent dye from its red-aggregated to its green-monomeric forms (Figure 4A, left panels). Specifically, a majority (97.8%) of solvent-treated KU812 cells had a bright red fluorescence, indicative of intact mitochondria, while 35.3% of **10**-treated KU812 cells at 100 nM for 8 h exhibited a marked green fluorescence indicative of damaged mitochondria. Nuclear morphology of **10**-treated KU812 cells was also evaluated using Hoechst-3258 staining (Figure 4B, right panels); a blue-to-cyan fluorescence was detected in most of the nuclei of **10**-treated *vs* DMSO-control cells indicating their apoptotic morphology. Taken together, these data indicated that **10** significantly decreased CML proliferation by inducing G2/M phase arrest and apoptosis via a mitochondria-dependent pathway.

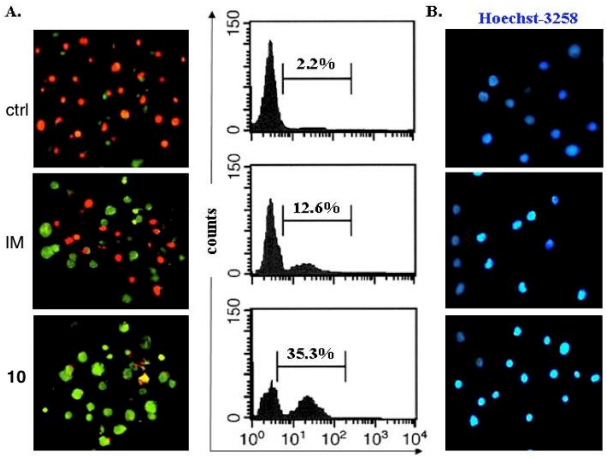

Figure 4. Compound **10** promotes CML cell death via mitochondrial-dependent pathways – comparsion with IM. Experiments were performed in triplicate.

We examined the ability of **10** to augment the cytotoxic effects of IM in human CML cells. To study this, LAMA84 cells were incubated for 48 h with increasing doses of IM (range 1-1000 nM) in the absence or presence of 100 nM **10** and then analyzed by the MTT assay (Figure 5A). The combined regimen of IM and **10** was more effective than IM alone in reducing CML cell growth, lowering the IC_{50} value for IM from 100 nM to less than 10 nM. It had been reported previously that the average IC_{50} value for IM in LAMA84 cells overexpressing BCR-ABL is 100 nM,[4] and this was also observed here. Similar results were also obtained using KU812 cells (data not shown). In addition, the IM-resistant KBM5-T315I cells showed the same susceptibility to **10**-induced cell death as well as IM-sensitive KBM5-WT cells, reaching respectively 58.2 ± 4.5% and 62.6 ± 5.4% of annexin V^+ cells at 48 h of drug exposure as compared to 2.2 ± 1.8% for control cells. Most importantly, exposure to 100 nM **10** significantly augmented the pro-apoptogenic effects of IM, when annexin V-FITC staining was used to detect early cell death at 24 h (Figure 5B).

Given that **10** interferes with tubulin function, we then examined cell morphological features under phase contrast microscopy and cell cycle distribution by flow cytometry (Figure 1S, Supporting Information). Compared to cell cultures incubated with DMSO as vehicle control (ctrl), KU812 cells treated with 100 nM **10** showed an elongated shape and multiple centrosomes typical of giant cells with failed cytokinesis and altered tubulin immunostaining (Figure 1S, Panel A).

These characteristics, typically resembling those referred to as mitotic catastrophe, occurred at relatively early (2 to 8 h) exposure intervals correlating with a net mitotic arrest of **10**-treated cells accumulated in the G_2/M cell cycle phase (60.3 ± 3.4% of treated *vs* 35.7 ± 2.8% of control cells), whereas apoptotic cells in the subG_1 phase did not exceed 10%. After a 24 h treatment, cell mitotic abnormalities disappeared in keeping with a reduced G_2/M fraction reaching 11.4 ± 8.3%, whilst a massive apoptosis induction (peaking at 75.6 ± 11.4% of **10**-treated cells *vs* 0.4 ± 0.8% of control cells) indicated a greater susceptibility to death following the initial mitotic arrest (Figure 1S, Panel B).

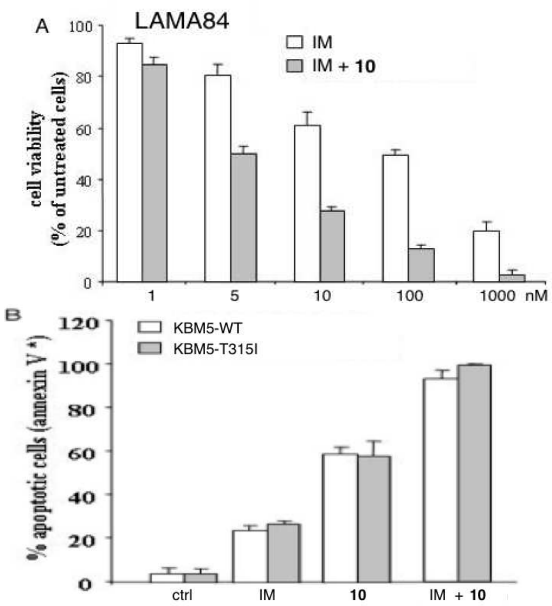

Figure 5. Compound **10** potentiates IM-mediated cell death of CML cells, including those expressing the T315I mutation. Experiments were performed in triplicate.

It is worth noting that IM, when used as a single agent at 100 nM, was ineffective in altering CML KU812 cell shape or viability, causing only a weak anti-proliferative effect at 24 h (56.3 ± 3.4% in IM-treated *vs* 42.7 ± 6.2% in DMSO-treated cells arrested in the G_1 phase of the cell cycle). As shown in Figure 1S, Panel C, the levels of the growth inhibitory protein $p21^{Cip/WAF1}$ were rapidly up-regulated after 6 h of **10** treatment and decreased after 24 h when the cleavage of the pro-apoptotic protein PARP indicated prominent activation. In keeping with this

observation, treatment with **10** also increased caspase-3 activation in a time-dependent fashion, as assessed by flow cytometry (Figure 1S, Panel D).

To determine whether **10** interferes with BCR/ABL phosphoactivation and its signal transduction machinery, LAMA84 cells were cultured for 24 h in the presence of IM or **10**, both at 100 nM. Cells were then lysed and analyzed by Western immunoblotting (Figure 2S, Supporting Information). Treatment with **10** did not alter auto-activation, while total levels of E-cadherin were substantially reduced compared to cells incubated with DMSO or IM. Compound **10** also reduced the active pools of unphosphorylated β-catenin and phospho-cofilin without affecting their total protein levels. Since β-catenin and cofilin act as cytoskeletal adaptor proteins and are critical determinants of CML cell growth, it seems conceivable that these two molecules may elicit the anti-leukemic potential of **10**, beyond its expected effects on tubulin function.

In conclusion, we synthesized ARDAP derivatives as potential anticancer agents. The new ARDAPs inhibited tubulin polymerization with IC_{50} values in the micro- or submicromolar concentration range. Most compounds inhibited the proliferation of human MCF-7 cells with IC_{50} values ≤30 nM. The most potent MCF-7 cell growth inhibitor within the series, **10** (IC_{50} = 9 nM), proved to inhibit BCR/ABL-expressing KU812 and LAMA84 cells from CML patients in blast crisis and hematopoietic cells ectopically expressing the IM-sensitive KBM5-WT or its IM-resistant KBM5-T315I mutation. The CML cell inhibition went through G2/M phase arrest and apoptosis via a mitochondria-dependent pathway. ARDAP **10** augmented the cytotoxic effects of IM in human CML cells. IM and **10** in combination improved the effectiveness of IM alone in reducing CML cell growth, with a 10-fold decrease in the IC_{50} value for IM, from 100 nM to less than 10 nM. Overall, our results indicate that compound **10** has potential as a novel drug to treat CML. On the basis of this valuable information, new ARDAP compounds are currently being synthesized with guidance from computational studies, and the results will be reported in due course.

ASSOCIATED CONTENT

Supporting Information

The Supporting Information is available free of charge on the ACS Publications website.

Additional biological information, experimental procedures for the synthesis and characterization of **4-16**, molecular modeling and biological assays (pdf file).

AUTHOR INFORMATION

Corresponding Author

***Phone: +39 06 4991 3800. Fax: +39 06 4991 3133. E-mail: romano.silvestri@uniroma1.it.**

Author Contributions

G.L.R, V.F., S.P. and M.N.: chemical synthesis; A.C. and A.B.: molecular modeling studies; R.B. and E.H.: tubulin studies and MCF-7, OVCAR-8 and NCI/ADR-RES cell growth inhibition; C.S. and A.M.L.C: biological screenings.

Funding Sources

This research was supported by grants PRIN 2015 n. 2015FCHJ8E (R.S.), AIRC-IG n. IG.14236 (A.M.L.C.), Ricerche Universitarie 2015 Sapienza Università di Roma n. C26A15J3BB (G.L.R.) and n. C26A15RT82 (A.C.) and Finanziamenti Ateneo 2016 Sapienza Università di Roma (G.L.R.).

Notes

The authors declare no competing financial interest.

Disclaimer

The content of this paper is solely the responsibility of the authors and does not necessarily reflect the official views of the National Institutes of Health.

ABBREVIATIONS

ARDAP, 3-aroyl-1,4-diarylpyrrole; CML, chronic myeloid leukemia; BCR, breakpoint cluster region; ABL, abelson gene; BCR/ABL fusion gene; ATI, arylthioindole; ARAP, 3-aroyl-1-arylpyrrole; CSA4, combretastatin A-4; TosMIC, *p*-toluenesulfonylmethyl isocyanide; DCE, 1,2-dichloroethane; PBMC, peripheral blood mononuclear cell; IM, imatinib mesylate.

REFERENCES

(1) NCI, SEER Stat Fact Sheets: Chronic Myeloid Leukemia (CML), accessed on 10/07/2016.

(2) Apperley, J. F. Chronic myeloid leukaemia. *Lancet* **2015**, *385*, 1447–1459.

(3) Marin, D.; Rotolo, A.; Milojkovic, D.; Goldman, J. The next questions in chronic myeloid leukaemia and their answers. *Curr. Opin. Hematol*. **2013**, *20*, 163–168.

(4) Walz, C.; Sattler, M. Novel targeted therapies to overcome imatinib mesylate resistance in chronic myeloid leukemia (CML). *Crit. Rev. Oncol./Hematol*. **2006**, *57*, 145–164.

(5) Wei, Y.; Hardling, M.; Olsson, B.; *et al.* Not all imatinib resistance in CML are BCR-ABL kinase domain mutations. *Ann. Hematol*. **2006**, 85, 841–847.

(6) le Coutre, P.; Tassi, E.; Varella-Garcia, M.; *et al.* Induction of resistance to the Abelson inhibitor STI571 in human leukemic cells through gene amplification. *Blood* **2000**, *95*, 1758–1766.

(7) Pagnano, K. B.; Bendit, I.; Boquimpani, C.; *et al.* Bengió, 5 on behalf of Latin American Leukemia Net Lalnet RM. BCR-ABL mutations in chronic myeloid leukemia treated with tyrosine kinase inhibitors and impact on survival. *Cancer Invest*. **2015**, *33*, 451–458.

(8) de Bruin, E. C.; Medema, J. P. Apoptosis and non-apoptotic deaths in cancer development and treatment response. *Cancer Treat. Rev*. **2008**, *34*, 737–749.

(9) Teicher, B. A. Newer cytotoxic agents: attacking cancer broadly. *Clin. Cancer Res.* **2008**, *14*, 1610–1617.

(10) Bates, D.; Feris, E. J.; Danilov, A. V.; Eastman, A. Rapid induction of apoptosis in chronic lymphocytic leukemia cells by the microtubule disrupting agent BNC105. *Cancer Biol. Ther.* **2016**, *17*, 291–299.

(11) Ducki, S.; Rennison, D.; Woo, *et al.* Combretastatin-like chalcones as inhibitors of microtubule polymerization. Part 1: synthesis and biological evaluation of antivascular activity. *Bioorg. Med. Chem.* **2009**, *17*, 7698–7710.

(12) Ducki, S.; Forrest, R.; Hadfield, J. A.; Kendall, A.; *et al.* Potent antimitotic and cell growth inhibitory properties

of substituted chalcones. *Bioorg. Med. Chem. Lett.* **1998**, *8*, 1051–1056.
(13) Cao, R.; Wang, Y.; Huang, N. Discovery of 2-acylaminothiophene-3-carboxamides as multitarget inhibitors for BCR-ABL kinase and microtubules. *J. Chem. Inf. Model.* **2015**, *55*, 2435–2442.
(14) Rowinsky, E. K.; Donehower, R. C.; Jones, J. J.; Tucker, R. W. Microtubule changes and cytotoxicity in leukemic cell lines treated with taxol. *Cancer Res.* **1988**, *48*, 4093–4100.
(15) La Regina, G.; Sarkar T.; Bai, R.; Edler, M. C.; Saletti, R.; Coluccia, A.; Piscitelli, F.; Minelli, L.; Gatti, V.; Mazzoccoli, C.; Palermo, V.; Mazzoni, C.; Falcone, C.; Scovassi, A. I.; Giansanti, V.; Campiglia, P.; Porta, A.; Maresca, B.; Hamel, E.; Brancale, A.; Novellino, E.; Silvestri, R. New arylthioindoles and related bioisosteres at the sulfur bridging group. 4. Synthesis, tubulin polymerization, cell growth inhibition, and molecular modeling studies. *J. Med. Chem*. **2009**, *52*, 7512–7527.
(16) La Regina, G.; Bai, R.; Coluccia, A.; Famiglini, V.; Pelliccia, S.; Passacantilli, S.; Mazzoccoli, C.; Ruggieri, V.; Sisinni, L.; Bolognesi, A.; Rensen, W. M.; Miele, A.; Nalli, M.; Alfonsi, R.; Di Marcotullio, L.; Gulino, A.; Brancale, A.; Novellino, E.; Dondio, G.; Vultaggio, S.; Varasi, M.; Mercurio, C.; Hamel, E.; Lavia, P.; Silvestri, R. New pyrrole derivatives with potent tubulin polymerization inhibiting activity as anticancer agents including Hedgehog-dependent cancer. *J. Med. Chem.* **2014**, *57*, 6531–6552.
(17) Nguyen, T. L.; McGrath, C.; Hermone, A. R.; Burnett, J. C.; Zaharevitz, D. W.; Day, B. W.; Wipf, P.; Hamel, E.; Gussio, R. A common pharmacophore for a diverse set of colchicine site inhibitors using a structure-based approach. *J. Med. Chem.* **2005**, *48*, 6107−6116.
(18) La Regina, G.; Bai, R.; Rensen, W. M.; Di Cesare, E.; Coluccia, A.; Piscitelli, F.; Famiglini, V.; Reggio, A.; Nalli, M.; Pelliccia, S.; Da Pozzo, E.; Costa, B.; Granata, I.; Porta, A.; Maresca, B.; Soriani, A.; Iannitto, M. L.; Santoni, A.; Li, J.; Cona, M. M.; Chen, F.; Ni, Y.; Brancale, A.; Dondio, G.; Vultaggio, S.; Varasi, M.; Mercurio, C.; Martini, C.; Hamel, E.; Lavia, P.; Novellino, E.; Silvestri, R. Toward highly potent cancer agents by modulating the C-2 group of the arylthioindole class of tubulin polymerization inhibitors. *J. Med. Chem.* **2013**, *56*, 123–149.

TOC Graphic

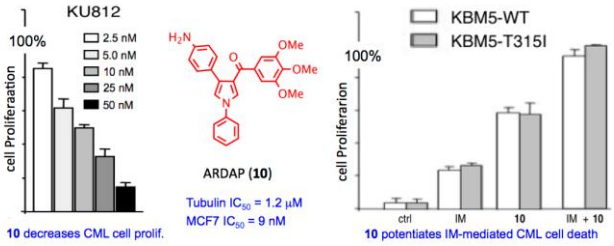
KU812
100%
2.5 nM
5.0 nM
10 nM
25 nM
50 nM
cell Proliferaation
10 decreases CML cell prolif.
H2N
O
OMe
OMe
OMe
N
ARDAP (10)
Tubulin IC50 = 1.2 μM
MCF7 IC50 = 9 nM
KBM5-WT
KBM5-T315I
100%
cell Proliferarion
ctrl
IM
10
IM + 10
10 potentiates IM-mediated CML cell death